Interaction of Rh(I) with *meso*-Arylsapphyrins and -Rubyrins: First Structural Characterization of Bimetallic Hetero-rubyrin Complex†

Seenichamy Jeyaprakash Narayanan, Bashyam Sridevi, and Tavarekere K. Chandrashekar*

Department of Chemistry, Indian Institute of Technology, Kanpur 208016, India

Ulrich Englich and Karin Ruhlandt-Senge

Department of Chemistry, Syracuse University, Syracuse, New York 13244

Received June 27, 2000

The ligational behavior of *meso*-arylsapphyrins and rubyrins toward Rh(I) is investigated. Sapphyrins form monometallic complexes with coordination of one imine and amine type nitrogens of the bipyrrole unit in an η^2 fashion. The Rh(I) coordination is completed by the presence of two ancillary carbon monoxide ligands. Rubyrins form both monometallic and bimetallic complexes. Two types of bimetallic complexes have been isolated. In the first type, both rhodium atoms are projected above the mean rubyrin plane, while in the second type, one rhodium atom is projected above and the other below the mean plane. Detailed ^{1}H and 2D NMR spectral analyses along with IR and UV−visible spectra of the complexes confirm the proposed binding modes for the rhodium complexes. Furthermore, the single-crystal X-ray analysis of one of the bimetallic complexes of rubyrin shows a bowl-shaped symmetric structure where both Rh(I) atoms are projected above the mean rubyrin plane at an angle of 71.73°. The geometry around each rhodium center is approximately square planar [N1−Rh1−N2, 80.38(9)°; C15−Rh1−C16, 86.95(14)°; N1−Rh1−C15, 97.13(12)°; and N2−RH1−C16, 94.97(12)°]. The *o*bserved distance of 4.313 Å between the two rhodium centers reveals very little interaction between the two rhodium atoms. This type of metal binding is accompanied by a 180° ring flip of the heterocyclic ring connecting the two bipyrrole units. In dioxarubyrin, where one of the pyrrole rings of the bipyrrole unit is inverted, Rh(I) binds at the periphery to the pyrrole nitrogen, leaving the rubyrin cavity empty. The absence of one amino and one imino nitrogen on the dipyrromethene subunits in the sapphyrins and rubyrins described here forces Rh(I) to bind to bipyrrole nitrogens.

Introduction

Sapphyrin, **1**, and rubyrin, **2**, belong to the family of expanded

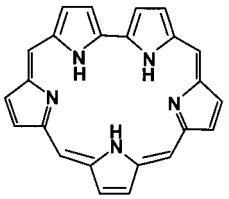

1

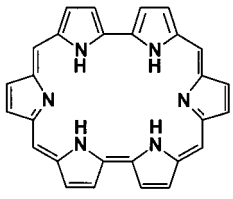

2

porphyrins and contain five and six pyrrole rings (heterocyclic rings), respectively.[1] Specifically, in sapphyrins, the five heterocyclic rings are linked in a cyclic manner through four meso carbon bridges in a 1.1.1.1.0 arrangement and they contain 22 conjugated π electrons. Rubyrins contain 26 π electrons, and the six heterocyclic rings are arranged in a 1.1.0.1.1.0 fashion with four methine bridges. After the early discovery of sapphyrins by Woodward and co-workers,[2] considerable progress has been made recently not only on syntheses of a range of sapphyrins but also on their rich and diverse chemistry.[3] Their receptor properties for anionic substrates,[4] structural diversity,[5] sapphyrin−nucleobase conjugates,[6] capped sapphyrins,[7] and heteroatom[3d,5] substitution have been exploited by various research groups.

β-Substituted rubyrin was first reported in 1991, and the X-ray structure of the protonated form is a planar structure.[8] On the other hand, the *meso*-arylrubyrins with heteroatoms show structural diversity where planar and inverted structures are reported.[9] Further, the substitution of one or more heteroatoms

† Dedicated to Prof. S. S. Krishnamurthy on the occasion of his 60th birthday.

* To whom correspondence should be addressed. E-mail: tkc@iitk.ac.in. Fax: 0091-512-597436/590007.

(1) Sessler, J. L.; Weghorn, S. J. In *The Porphyrin Handbook*; Kadish, K. M., Smith, K. M., Guilard, R., Eds.; Academic Press: San Diego, 2000; Vol. 2, pp 55−124.

(2) Bauer, V. J.; Clive, D. L. J.; Dolphin, D.; Paine, J. B., III.; Harris, F. L.; King, M. M.; Loder, J.; Wang, S. C.; Woodward, R. B. *J. Am. Chem. Soc.* **1983**, *105*, 6429−6436.

(3) (a) Broadhurst, M. J.; Grigg, R.; Johnson, A. W. *J. Chem. Soc., Perkin Trans. 1* **1972**, 2111−2116. (b) Sessler, J. L.; Cyr, M. J.; Lynch, V.; McGhee, E.; Ibers, J. A. *J. Am. Chem. Soc.* **1990**, *112*, 2810−2813. (c) Sessler, J. L.; Cyr, M. J.; Burrell, A. K. *Synlett* **1991**, 127−134. (d) Sessler, J. L.; Cyr, M. J.; Burrell, A. K. *Tetrahedron* **1992**, *48*, 9661−9672. (e) Sessler, J. L.; Lisowski, J.; Boudreaux, K. A.; Lynch, V.; Barry, J.; Kodadek, T. J. *J. Org. Chem.* **1995**, *60*, 5975−5978. (f) Paolesse, R.; Licoccia, S.; Spagnoli, M.; Boschi, T.; Khoury, R. G.; Smith, K. M. *J. Org. Chem.* **1997**, *62*, 5133−5137. (g) Sessler, J. L.; Hoehner, M. C.; Gebauer, A.; Andrievsky, A.; Lynch, V. *J. Org. Chem.* **1997**, *62*, 9251−9260. (h) Chmielewski, P. J.; Latos-Grazynski, L.; Rachlewicz, K. *Chem.−Eur. J.* **1995**, *1*, 68−72. (i) Bruckner, C.; Sternberg, E. D.; Boyle, R. W.; Dolphin, D. *Chem. Commun.* **1997**, 1689−1690. (j) Lash, T. D.; Richter, D. T. *J. Am. Chem. Soc.* **1998**, *120*, 9965−9966. (k) Srinivasan, A.; Mahajan, S.; Pushpan, S. K.; Kumar, M. R.; Chandrashekar, T. K. *Tetrahedron Lett.* **1998**, *39*, 1961−1964. (l) Narayanan, S. J.; Sridevi, B.; Srinivasan, A.; Chandrashekar, T. K.; Roy, R. *Tetrahedron Lett.* **1998**, *39*, 7389−7392. (m) Pushpan, S. K.; Narayanan, S. J.; Srinivasan, A.; Mahajan, S.; Chandrashekar, T. K.; Roy, R. *Tetrahedron Lett.* **1998**, *39*, 9249−9252.

10.1021/ic000703h CCC: $20.00
Published on Web 02/21/2001

alters the electronic structure of the ring, and this is reflected in the spectral properties. The anion receptor properties of a few rubyrins have also been reported very recently.[10]

Both sapphyrins and rubyrins contain heteroatoms in their core and therefore are expected to bind transition metals in their free base forms.[11] However, the coordination chemistry of sapphyrins and rubyrins is still in its infancy, where only a handful of metal complexes have been structurally characterized.[11] To the best of our knowledge, there are no reports on the metal binding properties of rubyrins to date while a few metal complexes of sapphyrins and hetero-sapphyrins containing first- and third-row transition metals have been characterized.[12] A summary of binding modes observed for sapphyrins is shown in Scheme 1. Only UO_2^{2+} complex of monooxasapphyrin is known to involve all the heteroatoms in the coordination mode as in **3a**.[12e] Most of the monometallic complexes exhibit binding as in **3b** where both in-plane and out-of-plane complexes have been characterized.[12a,c] In the bimetallic complexes, the metal atoms have been shown to bind as in **3c** where each metal atom is bridged between an imine and an amine nitrogen atom in an approximately square planar environment around each metal atom and where the metal planes are inclined at approximately 47° to the overall sapphyrin plane.[12a,b] The Co(II) ion coordinates to N5 sapphyrin involving four pyrrole nitrogens (as in **3e**),[2] and the corresponding Zn(II) complex switches between the symmetrical and unsymmetrical binding modes as in **3d** and **3e**.[3c]

Scheme 1 . Different Coordination Modes Reported for Metallosapphyrins

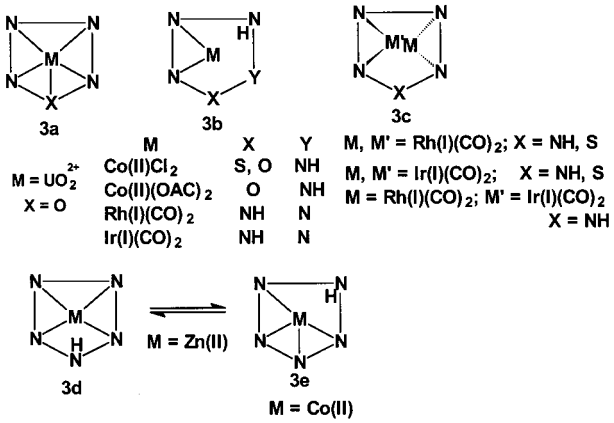

A few metal complexes of other expanded porphyrins such as pentaphyrin,[13] hexaphyrin,[14] amethyrin,[15] and oxasmaragdyrin have also been reported recently.[16] These studies have set the stage for thorough and systematic investigations on exploiting expanded porphyrins as ligands. In this paper we report the interaction of Rh(I) with a variety of hetero-sapphyrins and -rubyrins. New modes of binding other than those in the literature have been identified for hetero-sapphyrins, while for the first time it has been shown that the hetero-rubyrins act as ligands toward metals. In the monometallic complex, Rh(I) binds to two nitrogens of the same bipyrrole ring to form an out-of-plane complex in an η^2 fashion. Two types of out-of-plane bimetallic complexes, one having a bowl-shaped structure where both the metals are projected above the plane of the macrocycle and the second having one metal above and the other below the plane, have been isolated. Furthermore, it has been shown that the metal coordination in a particular mode is accompanied by a 180° ring flip of the heterocyclic rings connecting the two bipyrrole subunits. In dioxarubyrin where one of the pyrrole rings of the bipyrrole unit is inverted, Rh(I) binds only at the periphery coordinating to the pyrrole nitrogens of the inverted ring, leaving the cavity empty.

Results and Discussion

The modes of Rh(I) binding to the different sapphyrins and rubyrins are characterized by mass spectra and ^{1}H NMR, UV−

(4) (a) Sessler, J. L.; Andrievsky, A.; Genge, J. W. *Adv. Supramol. Chem.* **1997**, *4*, 97−142. (b) Sessler, J. L.; Burrell, A. K.; Furuta, H.; Hemmi, G. W.; Iverson, B. L.; Kral, V.; Magda, D. J.; Mody, T. D.; Shreder, K.; Smith, D.; Weghorn, S. J. *Transition Met. Supramol. Chem.* **1994**, 391−408. (c) Sessler, J. L.; Sansom, P. I.; Andrievsky, A.; Kral, V. In *Supramolecular Chemistry of Anions*; Bianchi, A., James, K. B., Espana, E. G., Eds.; Wiley-VCH: New York, 1997; pp 355−419. (d) Shionoya, M.; Furuta, H.; Lynch, V.; Harriman, A.; Sessler, J. L. *J. Am. Chem. Soc.* **1992**, *114*, 5714−5722. (e) Sessler, J. L.; Andrievsky, A.; Gale, P. A.; Lynch, V. *Angew. Chem., Int. Ed. Engl.* **1996**, *35*, 2782−2785. (f) Kral, V.; Furuta, H.; Shreder, K.; Lynch, V.; Sessler, J. L. *J. Am. Chem. Soc.* **1996**, *118*, 1595−1607. (g) Iverson, B. L.; Shreder, K.; Kral, V.; Sansom, P.; Lynch, V.; Sessler, J. L. *J. Am. Chem. Soc.* **1996**, *118*, 1608−1616. (h) Sessler, J. L.; Andrievsky, A.; Kral, V.; Lynch, V. *J. Am. Chem. Soc.* **1997**, *119*, 9385−9392. (i) Sessler, J. L.; Kral, V.; Genge, J. W.; Thomas, R. E.; Iverson, B. L. *Anal. Chem.* **1998**, *70*, 2516−2522.

(5) (a) Narayanan, S. J.; Sridevi, B.; Chandrashekar, T. K.; Vij, A.; Roy, R. *Angew. Chem., Int. Ed.* **1998**, *37*, 3394−3397. (b) Narayanan, S. J.; Sridevi, B.; Chandrashekar, T. K.; Vij, A.; Roy, R. *J. Am. Chem. Soc.* **1999**, *121*, 9053−9068. (c) Srinivasan, A.; Anand, V. G.; Narayanan, S. J.; Pushpan, S. K.; Kumar, M. R.; Chandrashekar, T. K.; Sugiura, K.; Sakata, Y. *J. Org. Chem.* **1999**, *64*, 8693−8697. (d) Srinivasan, A.; Pushpan, S. K.; Kumar, M. R.; Mahajan, S.; Chandrashekar, T. K.; Roy, R.; Ramamurthy, P. *J. Chem. Soc., Perkin Trans 2* **1999**, 961−968. (e) Srinivasan, A.; Anand, V. G.; Pushpan, S. K.; Chandrashekar, T. K.; Sugiura, K.; Sakata, Y. *J. Chem. Soc., Perkin Trans 2* **2000**, 1788−1793.

(6) (a) Kral, V.; Sessler, J. L.; Furuta, H. *J. Am. Chem. Soc.* **1992**, *114*, 8704−8705. (b) Sessler, J. L.; Furuta, H.; Kral, V. *Supramol. Chem.* **1993**, *1*, 209−220. (c) Kral, V.; Sessler, J. L. *Tetrahedron* **1995**, *51*, 539−554. (d) Sessler, J. L.; Sansom, P. I.; Kral, V.; O'Connor, D.; Iverson, B. L. *J. Am. Chem. Soc.* **1996**, *118*, 12322−12330. (e) Sessler, J. L.; Andrievsky, A. *Chem. Commun.* **1996**, 1119−1120.

(7) (a) Sessler, J. L.; Brucker, E. A.; Kral, V.; Harriman, A. *Supramol. Chem.* **1994**, *4*, 35−41. (b) Sessler, J. L.; Brucker, E. A. *Tetrahedron Lett.* **1995**, *36*, 1175−1176.

(8) Sessler, J. L.; Morishima, T.; Lynch, V. *Angew. Chem., Int. Ed. Engl.* **1991**, *30*, 977−980.

(9) (a) Narayanan, S. J.; Srinivasan, A.; Sridevi, B.; Chandrashekar, T. K.; Senge, M. O.; Sugiura, K.; Sakata, Y. *Eur. J. Org. Chem*. **2000**, 2357−2360. (b) Srinivasan, A.; Pushpan, S. K.; Kumar, M. R.; Chandrashekar, T. K.; Roy, R. *Tetrahedron* **1999**, *55*, 6671−6680.

(10) (a) Srinivasan, A.; Reddy, M. V.; Narayanan, S. J.; Sridevi, B.; Pushpan, S. K.; Kumar, M. R.; Chandrashekar, T. K. *Angew. Chem., Int. Ed. Engl.* **1997**, *36*, 2598−2601. (b) Furuta, H.; Morishima, T.; Kral, V.; Sessler, J. L. *Supramol. Chem.* **1993**, *3*, 5−8. (c) Srinivasan, A.; Anand, V. G.; Pushpan, S. K.; Chandrashekar, T. K.; Sugiura, K.; Sakata, Y. *J. Chem. Soc., Perkin Trans. 2* **2000**, 1788−1793.

(11) (a) Sessler, J. L., Weghorn, S. J., Eds. In *Expanded, Contracted & Isomeric Porphyrins*; *Tetrahedron Organic Chemistry Series, Vol. 15*; Pergamon: New York, 1997. (b) Jasat, A.; Dolphin, D. *Chem. Rev.* **1997**, *97*, 2267−2340.

(12) (a) Burrell, A. K.; Sessler, J. L.; Cyr, M. J.; McGhee, E.; Ibers, J. A. *Angew. Chem., Int. Ed. Engl.* **1991**, *30*, 91−93. (b) Lisowski, J.; Sessler, J. L.; Lynch, V. *Inorg. Chem.* **1995**, *34*, 3567−3572. (c) Sessler, J. L.; Burrell, A. K.; Lisowski, J.; Gebauer, A.; Cyr, M. J.; Lynch, V. *Bull. Soc. Chim. Fr.* **1996**, *133*, 725−734. (d) Burrell, A. K.; Cyr, M. J.; Lynch, V.; Sessler, J. L. *Chem. Commun.* **1991**, 1710−1713. (e) Sessler, J. L.; Gebauer, A.; Hoehner, M.; Lynch, V. *Chem. Commun.* **1998**, 1835−1836.

(13) (a) Gossauer, A. *Chimia* **1984**, *38*, 45−46. (b) Burrell, A. K.; Hemmi, G.; Lynch, V.; Sessler, J. L. *J. Am. Chem. Soc.* **1991**, *113*, 4690−4692. (c) Kral, V.; Brucker, E. A.; Hemmi, G.; Sessler, J. L.; Kralova, J.; Bose, H. *J. Bioorg. Med. Chem.* **1995**, *3*, 573−578.

(14) Charriere, R.; Jenny, T. A.; Rexhausen, H.; Gossauer, A. *Heterocycles* **1993**, *36*, 1561−1575.

(15) (a) Sessler, J. L.; Weghorn, S. J.; Hiseada, Y.; Lynch, V. *Chem.*−*Eur. J.* **1995**, *1*, 56−67. (b) Weghorn, S. J.; Sessler, J. L.; Lynch, V.; Baumann, T. F.; Sibert, J. W. *Inorg. Chem.* **1996**, *35*, 1089−1090. (c) Sessler, J. L.; Gebauer, A.; Scherer, M.; Lynch, V. *Inorg. Chem.* **1998**, *37*, 2703−2706.

(16) Sridevi, B.; Narayanan, S. J.; Chandrashekar, T. K.; Englich, U.; Senge, K. R. *Inorg. Chem.* **2000**, *39*, 3669−3677.

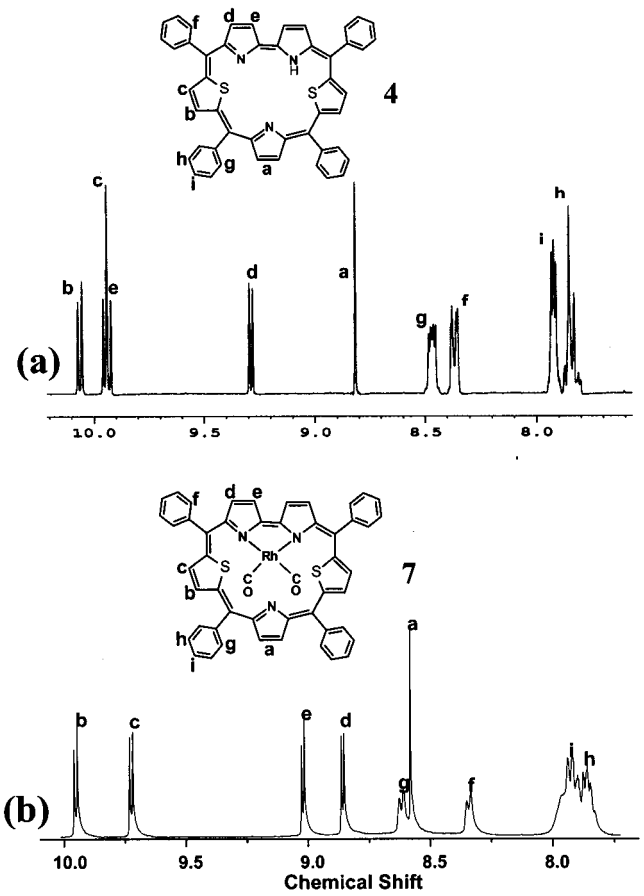

Figure 1. ^{1}H NMR ($CDCl_3$) spectra of **4** (a) and **7** (b).

Scheme 2 . Synthesis of Rh(I) Complex of Modified Sapphyrins

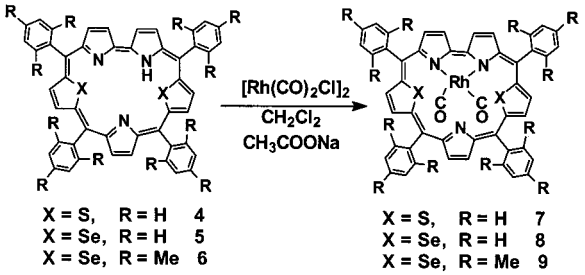

visible, and IR methods. The single-crystal X-ray structure of one of the bimetallic complexes of rubyrin further confirms the suggested mode of binding.

Scheme 2 shows the metal coordination to three sapphyrins, **4**, **5**, and **6**. Rhodium binds to two bipyrrole nitrogens in a η^2 fashion as in **7**−**9**, and the coordination is completed by the presence of two carbonmonoxide ligands in an approximate square planar geometry. This mode of binding is arrived at by a comparison of ^{1}H NMR spectra of free base **4** and the rhodium complex **7** shown in Figure 1. In **4**, the bipyrrole protons d, d′ and e, e′ are equivalent among themselves because of the rapid tautomerism at room temperature of the inner hydrogen between the two bipyrrole nitrogens, resulting in the presence of a symmetry axis passing between the bipyrrole ring and the opposite pyrrole ring.[5b,17] When the temperature is lowered, the

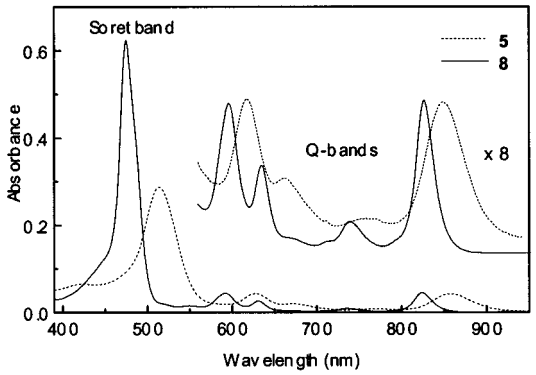

Figure 2. UV−visible spectra for **5** (2.126×10^{-6} M) and **8** (5.276×10^{-6} M) in CH_2Cl_2 in the Soret and Q-band regions.

pyrrole proton is localized on one of the bipyrrole nitrogens, destroying the symmetry that results in the appearance of individual doublets for each proton. The metal coordination as in **7** also results in the presence of a symmetry axis, and as a result of this, one would expect that the ^{1}H NMR spectrum of **7** should be similar to that of **4** at room temperature. This is exactly what has been observed. The metal coordination results in the shifts of specific protons. The bipyrrole protons d and e experience a significant shielding upon metal coordination [0.43 and 0.91 ppm for **7**, 0.37 and 0.85 for **8**, and 0.19 and 0.62 for **9**], while the thiophene protons c and b and pyrrole protons a, whose heteroatoms are not involved in the coordination to the metal, experience small shifts. This observation is in agreement with the earlier literature reports.[12,16,18] This mode of metal binding is different from other hetero-sapphyrins reported in the literature. In general the metal binds to one imine and amine type of nitrogen present on the dipyrromethene subunit of the sapphyrin.[12,16] But in the present case, lack of one imine and one amine type nitrogen on the dipyrromethene subunit due to the presence of heteroatom, the metal is forced to bind to the imine and amine type of nitrogen present on the bipyrrole unit.

The UV−visible spectra of **5** and **8** shown in Figure 2 also confirm the metal coordination. Both the Soret and Q bands experience red shifts upon metal binding (for **7**−**9** Soret and Q-band shifts are 35−40 nm and 25−30 nm, respectively), which is consistent with the earlier reports.[12c,19]

The metal binding mode of **10** is shown in Scheme 3. **10** shows an unusual inverted structure where one of the pyrrole rings of each bipyrrole unit is inverted and there is a slow flipping of these rings at room temperature, giving rise to broad ^{1}H NMR resonances.[9a] Because of this ring inversion, the pyrrole −NH protons are localized; hence, there is no tautomerism possible. This is confirmed by the appearance of a pyrrole −NH signal in the shielded region (−2.5 ppm) at room temperature. A comparison of ^{1}H NMR spectra of **10** and its metal derivatives is made in Figure 3. The peak assignments that are marked are based on correlations observed in ^{1}H−^{1}H correlation spectroscopy (COSY). An inspection of the figure indicates (a) sharpening of the resonances upon metal binding, (b) doubling of the resonances where all the peaks appear in pairs, and (c) the appearance of peaks for the inner pyrrole −NH protons (g, g′) in the shielded region. The sharpening of the

(17) (a) Rachlewicz, K.; Sprutta, N.; Latos-Grazynski, L.; Chmielewski, P. J.; Szterenberg, L. *J. Chem. Soc., Perkin Trans.* **1998**, 959−967. (b) Rachlewicz, K.; Sprutta, N.; Chmielewski, P. J.; Latos-Grazynski, L. *J. Chem. Soc., Perkin Trans.* **1998**, 969−975.

(18) It is documented in the literature that the β-CH protons of the ring experience significant shielding upon metal binding to the heteroatom of the ring. If the heteroatom is not involved in coordination, the β-CH protons experience a deshielding.

(19) (a) Ravikanth, M.; Chandrashekar, T. K. *Struct. Bonding* **1995**, *82*, 105−188. (b) Gouterman, M. In *The Porphyrins*; Dolphin, D., Ed.; Academic Press: New York, 1978; Vol. III, pp 1−165.

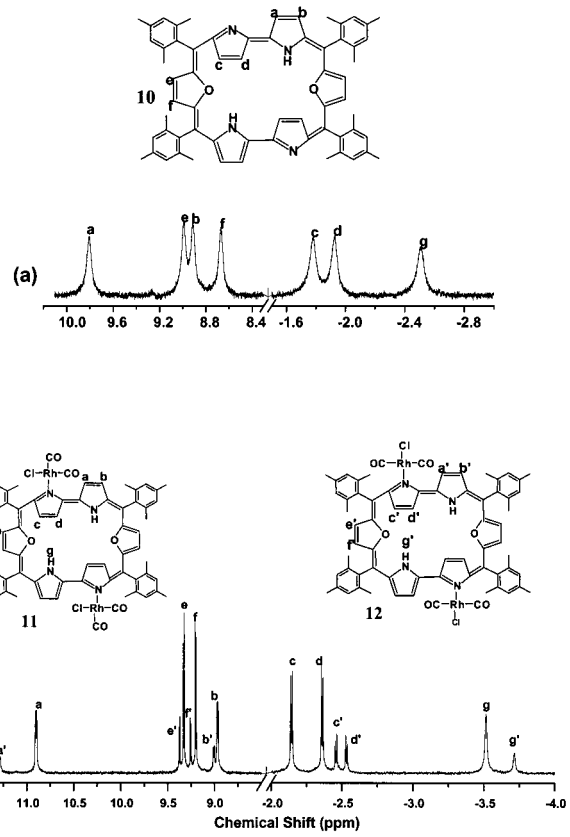

Figure 3. ^{1}H NMR ($CDCl_3$) spectra of **10** (a) and **11** and **12** (b).

Scheme 3 . Synthesis Scheme for Rh(I) Interaction with Dioxarubyrins

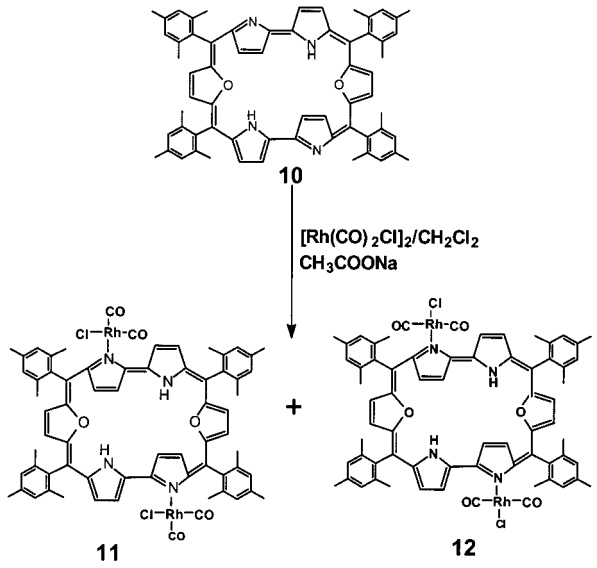

resonances upon metal binding suggests that the flipping of one of the pyrrole rings of bipyrrole units observed for the free base **10** is no longer present in the complex. The appearance of peaks for the inner pyrrole −NH protons (g, g′) in the shielded region rules out the metal coordination inside the rubyrin cavity. This leads us to suggest that the metal is bound to the pyrrole nitrogen of the inverted ring as shown in **11** and **12**, and the mass spectra confirmed the presence of two rhodium atoms in the complex. The doubling of resonances for all the protons suggests the presence of two species in solution that do not interconvert into one another on the NMR time scale. We identify these species as isomers **11** and **12**, and our attempts to separate these isomers

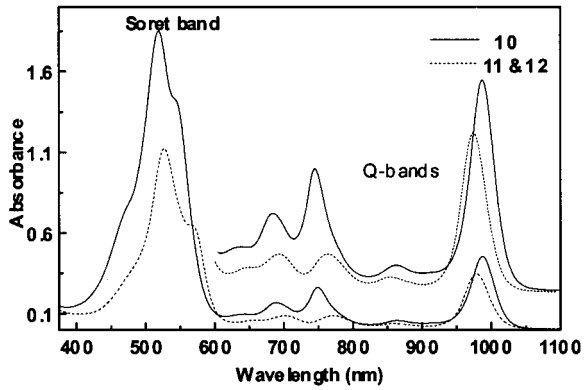

Figure 4. UV−visible spectra for **10** (3.934×10^{-6} M) and **11** and **12** (12.27×10^{-6} M) in CH_2Cl_2 in the Soret and Q-band regions.

Scheme 4 . Synthesis of Mono- and Bimetallic Rh(I) Complexes of Heteroatom Rubyrins

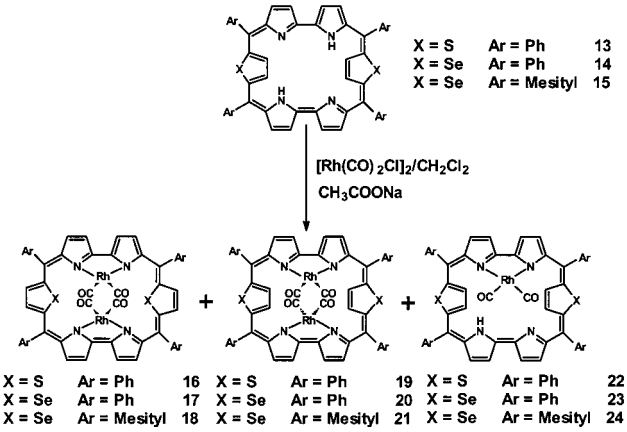

proved to be futile. Significant shielding of c and d protons (0.24 and 0.36 ppm for cc′ protons and 0.56 and 0.54 ppm for dd′ protons) and deshielding of a and b protons (0.94 and 1.42 ppm for aa′ and 0.54 and 0.6 ppm for bb′ protons) upon metal coordination further support the suggested binding mode. Also, the appearance of these protons as quartets suggests the presence of three-bond coupling between the −NH protons and the a and b protons [$^3J = 2$ Hz]. The e and f protons, which are away from the metal center, experience minimum shifts upon metal binding. The two isomers **11** and **12** are different only with respect to the presence of CO ligands in cis and trans geometry with respect to the rhodium atom. This mode of periphery metal binding is very unusual and is somewhat similar to that proposed for Pd^{2+} binding to the isomeric mixture of hexaphyrins[14] where the two pyrrole rings rotate outward by 180° prior to the coordination to form the periphery-bound Pd^{2+} hexaphyrin complex. The UV−visible spectra (Figure 4) further confirm the formation of metal complexes. Small shifts (8 nm for Soret band and ∼10−12 nm for Q bands) are observed upon metal binding in the electronic spectrum. However, the magnitude of observed shifts are much smaller than those observed for heterosapphyrins, confirming the metal ion binding at the periphery rather than inside the cavity.[12]

Reaction of 2 equiv of $[Rh(CO)_2Cl]_2$ with free base rubyrins **13**, **14**, and **15** in dichloromethane for about 20−30 min gave a mixture of products (Scheme 4) containing both mono- and bimetallic complexes. The major product monometallic complexes **22**, **23**, and **24** were isolated in about 25−30% yield. Two types of bimetallic complexes were isolated; complexes **16**, **17**, and **18** in ∼6% yield and complexes **19**, **20**, and **21** in

~1% yield. These mixtures of products can be easily separated on the column because of their differing polarity. In a typical reaction, **16** came first as a blue band followed by **19** (violet band) and **22** (came last as a magenta band).

In monometallic complexes the Rh(I) binds to two nitrogens of the same bipyrrole unit, forming an out-of-plane complex. Furthermore, the heterocyclic rings linking the two bipyrrole units remain inverted as in the corresponding free bases. In the bimetallic complexes each Rh(I) also binds to two nitrogens of a bipyrrole unit in an η^2 fashion but the difference between the two types, being in one case as in **16**, is that both rhodium atoms are pointing above the plane of the macrocycle, and this type of coordination is accompanied by a 180° ring flip of the heterocyclic ring linking the two bipyrrole units. In the second case, as in **19**, the two rhodium atoms are in two different planes where one rhodium is projected above and the other one below the mean rubyrin plane. In this type of binding the heterocyclic ring linking the two bipyrrole units remain inverted as in the corresponding free base.

The proposed structures for complexes **16**−**24** are based on the structural data available in the literature for the Rh(I) complexes of hetero-sapphyrins[12] and amethyrin[15c] as well as on the single-crystal X-ray structure of the complex **16** (vide infra). In the bis-Rh(I) complexes of heterosapphyrins, the metal binds to two nitrogens of dipyrromethane subunits such that one rhodium atom is projected above and the other rhodium is projected below the mean sapphyrin plane with an approximately square planar arrangement around each metal center.[12b,c] In amethyrin, the X-ray structure of the bis-rhodium complex is a bowl-shaped structure where both the metals are projected above the plane of the amethyrin skeleton, imparting a symmetry to the complex.[15c] However, in solution, variable-temperature proton NMR studies reveal the presence of two species where in one case both the rhodium atoms are projected above the plane of the macrocycle as in the solid state. In the other species, the two rhodium atoms are found above and below the plane as in hetero-sapphyrins. It was not possible to separate the two species. However, in the present study, we were successful in the separation of two types of bimetallic complexes, and one of them has been structurally characterized.

Distinction between the Two Types of Bis-rhodium Complexes in Solution. An understanding of the ^{1}H NMR spectra of free base rubyrins is essential for distinguishing between the two types of metal complex structures. We have recently shown that the two heterocyclic rings connecting the two bipyrrole subunits in the hetero-rubyrins are rotating at room temperature, giving rise to broad, unresolved ^{1}H NMR signals.[5a,b] However, when the sample is cooled to −50 °C, this rotation can be arrested, and at this temperature the heterocyclic rings remain inverted, which has been confirmed by the presence of the β-CH proton signals of the inverted rings in the high-field region. Single-crystal X-ray structures also support such a conclusion.[5b]

A distinction between the two types of complexes can be made on the basis of the chemical shift of β-CH protons of the heterocyclic rings. If the heterocyclic ring is fully inverted, the β-CH protons should experience the ring current and are expected to resonate in the high-field region. If it is not inverted, these protons are expected to resonate in the aromatic region.[3h,5c] A comparison of ^{1}H NMR spectra of bis-rhodium complexes **17** and **20** made in Figure 5 clearly distinguishes between the two types.

The ^{1}H NMR spectra of **17** (Figure 5a) turned out to be very simple because of the presence of symmetry in the complex as

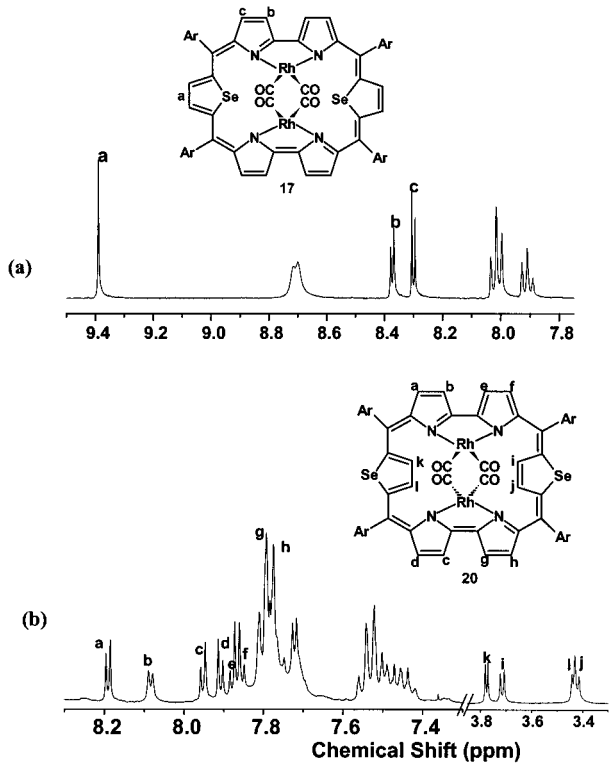

Figure 5. ^{1}H NMR ($CDCl_3$) spectra of **17** (a) and **20** (b).

revealed by X-ray structure analysis (vide infra). This makes the selenophene protons (a) equivalent, and they resonate as a sharp singlet at 9.39 ppm. Also, the bipyrrole protons (b and c) become equivalent and resonate as a doublet of doublet in the region 8.3−8.5 ppm. These assignments were confirmed by the correlations seen in the ^{1}H−^{1}H COSY results. Furthermore, the nonappearance of any peaks in the shielded region confirms the ring flipping upon rhodium coordination. The coordination of Rh(I) results in the characteristic shielding of bipyrrole protons relative to free base.[18] Similar spectra were observed for the complexes **16** and **18**.

In contrast, the spectra of **20** (Figure 5b) turned out to be quite complicated because of the presence of rhodium atoms above and below the mean rubyrin plane, destroying the symmetry. In this case, all 12 β-CH protons become inequivalent and resonate as individual doublets, suggesting the highly nonplanar nature of the complex. All the assignments marked in the spectrum are based on the correlations seen in the ^{1}H−^{1}H COSY. The important feature is the appearance of selenophene protons (i, j, k, and l) in the shielded region, suggesting that the ring inversion is retained upon metal binding. However, the chemical shifts observed for these protons suggest that the ring is not completely inside the plane of the macrocycle but is tilted slightly above such that these protons are away from the ring current region relative to the corresponding free base.

The ^{1}H NMR spectra of monometallic complex **24** is shown in Figure 6a. The mode of metal binding suggested here results in the formation of an out-of-plane rhodium complex, and the assignments marked are based on ^{1}H−^{1}H COSY (Figure 6b). The appearance of the selenophene protons (a and b) in the region −1.4 to −1.9 ppm clearly reveals that these rings are inverted as in the corresponding free base upon metal coordination. The rhodium coordination results in the typical shielding of bipyrrole protons (c and e) relative to bipyrrole protons (f and d) as observed for the rhodium sapphyrins **7**, **8**, and **9** (vide supra). Furthermore, the appearance of inner −NH proton (q)

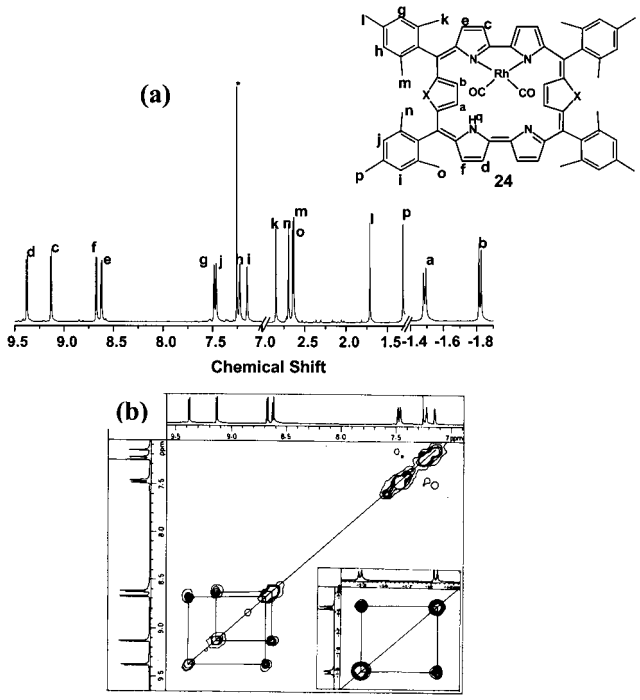

Figure 6. (a) ^{1}H NMR ($CDCl_3$) spectrum of **24** and (b) ^{1}H−^{1}H correlation spectrum ($CDCl_3$) of **24**.

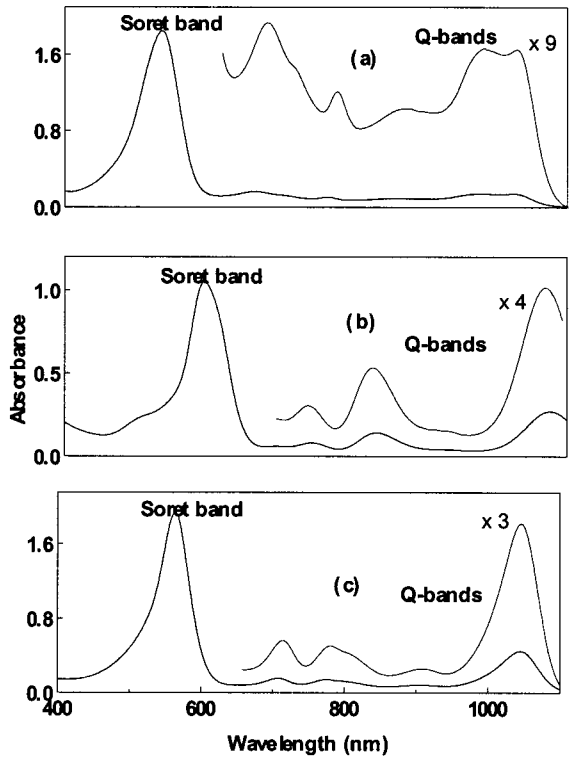

Figure 7. UV−visible spectra for **14** (14.179×10^{-6} M) (a), **17** (7.37×10^{-6} M) (b), and **23** (14.55×10^{-6} M) (c) in CH_2Cl_2 in the Soret and Q-band regions.

at −0.65 ppm at low temperature further confirms the mode of coordination. For complexes **22** and **23**, the peaks of selenophene appeared broader (line widths of ∼13 Hz) at room temperature, suggesting the flipping of the heterocyclic rings.

A comparison of UV−visible spectra of free base **14** and rhodium complexes **17** and **23** is made in Figure 7. In general, the metal complexation is accompanied by a red shift of both Soret and Q type bands. The magnitudes of shifts are smaller

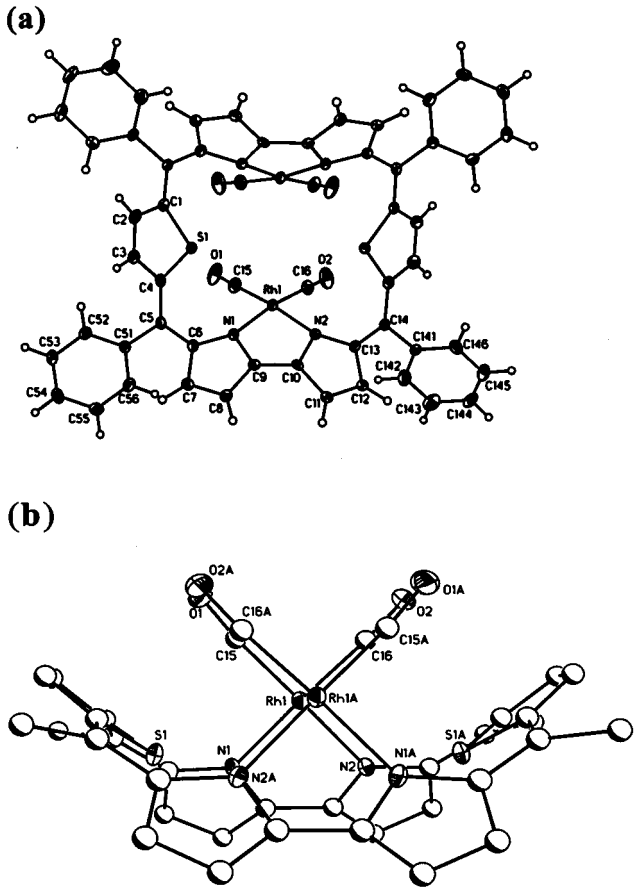

Figure 8. ORTEP diagram illustrating the cis orientation of two Rh(I) atoms in **16**: (a) plane view; (b) side view. Phenyl rings are omitted for clarity.

for monometallic complexes while higher for bimetallic complexes relative to the corresponding free base. For example, the monometallic complexes show a ∼30 nm red shift for the Soret band and a ∼22 nm shift for the Q type bands, while in the bimetallic complexes these shifts are ∼58 and 50 nm, respectively. These shifts are much larger compared to the shifts observed for dioxarubyrin metalation where the Rh(I) is coordinated at the periphery of the rubyrin. This kind of periphery coordination should not perturb the π electron delocalization, while the rhodium coordinated inside the rubyrin cavity is expected to perturb the delocalization pathway, and this is reflected in the larger optical absorption band shifts.[19]

X-ray Crystal Structure. The structure of complex **16** is shown in the Figure 8. The complex adopts a bowl-shaped structure in which both rhodium atoms are projected above the plane of the rubyrin skeleton and the coordination at the rhodium center is completed by the presence of two ancillary carbonyl ligands. Each rhodium atom is bound to one amine and one imine type of nitrogen present on the same bipyrrole unit. Furthermore, the two thiophene rings that link the two bipyrrole units have undergone a 180° ring flip relative to the corresponding free base upon Rh(I) coordination. This is reflected in drastic changes in the torsional angle S1−C4−C5−C6. For example, in free base rubyrin **14**,[5b] this angle was found to be −173.1(12)° while upon rhodium coordination this angle is reduced to −17.6°. The rhodium atoms are found 0.781 Å above the mean plane defined by the meso carbons, and the molecule is found to be symmetric. The metal plane (defined by N1, N2, Rh1, C15, C16, O1, and O2) is inclined by 71.73° (Figure 8, side view) with respect to the mean rubyrin plane, and this is

Table 1. Comparison of Selected Bond Lengths and Bond Angles for **16** and Dirhodium Complexes of Thiasapphyrin and Amethyrin

	complex **16**	dirhodium complex of thiasapphyrin[12c]	dirhodium complex of amethyrin[15c]
	Bond Length (Å)		
Rh1−N1	2.099(2)	2.083(2)	2.066(8)
Rh1−N2	2.087(2)	2.083(2)	2.054(7)
Rh1−C15	1.861(3)	1.847(3)	1.836(10)
Rh1−C16	1.851(3)	1.854(3)	1.869(11)
C9−C10	1.405(4)	1.434(4)	1.450(2)
Rh···Rh	4.313		4.1
	Bond Angle (deg)		
N1−Rh1−N2	80.38(9)	88.09(8)	85.8(3)
C15−Rh1−C16	86.95(14)	88.26(12)	89.4(4)
N1−Rh1−C15	97.13(12)	91.09(10)	91.5(4)
N2−Rh1−C16	94.97(12)	92.17(11)	92.5(4)

much higher than observed for metal sapphyrins (∼47°). The metal coordination results in the deviation of heterocyclic rings from the mean rubyrin plane constructed with four meso carbons. Specifically, the dihedral angles are 34.41° for thiophene ring, 48.12° for pyrrole ring containing N1, and 46.10° for pyrrole ring containing N2. The torsional angles C4−C5−C51−C52 and C1A−C14−C141−C146 are −37.5° and 56.3° and are found to be drastically reduced relative to those of the corresponding free base (65.0° and 57.6°), suggesting that the meso phenyl rings are almost coplanar with the rest of the macrocycle, increasing the delocalization pathway and justifying the red shifts observed upon metal coordination in the UV−vis spectra. The aromatic nature of the complexes is evident from the $C_\alpha-C_\beta$ distances (C6−C7, 1.434(4) Å; C8−C9, 1.411(4) Å) being longer than the $C_\beta-C_\beta$ distances (C7−C8, 1.360(4) Å).[8]

A comparison of relevant bond angles and bond distances observed for complex **16** along with bis-rhodium complexes of thiasapphyrin and amethyrin is made in Table 1. In general the Rh−N distances observed for **16** is slightly longer than observed for the corresponding sapphyrin and amethyrin complexes. The Rh−C distances of the CO ligand in all the cases are comparable, and the two rhodium atoms are well separated in **16**, suggesting that there is very little interaction between the two rhodium centers. A comparison of bond angles around the Rh(I) center reveals some interesting observations. Specifically, the N1−Rh1−N2 bond angle is more than 8° lower while the angle N1−Rh1−C15 is about 7° higher than observed for the corresponding bis-rhodium thiasapphyrin (Table 1). This is attributed to the difference in the coordination modes. In rubyrin complex **16** the metal is bound to two nitrogens of the bipyrrole unit, making the bond angle of N1−Rh1−N2 smaller at the expense of the bond angle N1−Rh1−C15, while in the thiasapphyrin complex the rhodium is bound to two nitrogens of the dipyrromethene unit. Furthermore, the effect of this mode of binding is reflected in significant lowering of the C9−C10 bond distance by 0.03 and 0.045 Å relative to the corresponding distances in the thiasapphyrin[12c] and amethyrin[15c] complexes, respectively.

Conclusions

The present results reveal that both *meso*-arylsapphyrins and -rubyrins can be used as ligands toward Rh(I). Generally, the heterosapphyrins reported in the literature form both monometallic and bimetallic complexes with Rh(I) by binding to nitrogens of dipyrromethene subunits. However, the sapphyrins described here contain one heteroatom (S or Se) in each dipyrromethene subunit, and hence, Rh(I) shows its preference in binding to nitrogen relative to S or Se by coordinating to bipyrrole nitrogens; this is limited to only monometallic complexes. The present study also describes for the first time, the coordination behavior of hetero-rubyrins and the formation of a bowl-like structure for the bimetallic complexes where both metals are pointing away from the mean plane in the same direction as in amethyrin,[15c] the second structure where metals are projected in two different planes as in hetero-sapphyrins[12] and where the formation of periphery-bound bimetallic complexes as in dioxarubyrin clearly highlights the versatility of rubyrin as a ligand. Furthermore, the 180° ring flip upon Rh(I) binding is quite unusual and suggests the flexibility of the ligand. The present study has exploited the interaction of only Rh(I), but other metal ions are also expected to interact with these macrocycles to form unique complexes that can further the domain of coordination chemistry of expanded porphyrins in general. Studies in this direction are in progress in this laboratory.

Table 2. Crystallographic Data for **16**

	16
solvent for crystallization	benzonitrile/methanol
empirical formula	$C_{56}H_{32}N_4O_4Rh_2S_2$
temp (K)	95(2)
cryst syst	monoclinic
space group	*C*2/*c*
vol (Å^3)	4517.64(12)
a (Å)	13.2046(2)
b (Å)	16.8107(3)
c (Å)	20.3873(3)
α (deg)	90
β (deg)	93.3860(10)
γ (deg)	90
Z	4
calcd density (g/cm^3)	1.610
reflns collected/unique	17354/5494
R(int)	0.0519
F(000)	2200
limiting indices	$-17 \le h \le 17$, $-22 \le k \le 16$, $-19 \le l \le 26$
GOF (F^2)	1.044
final *R* indices $\{I > 2\sigma(I)\}$	R1 = 0.0384, wR2 = 0.0776
R indices (all data)	R1 = 0.0609, wR2 = 0.0833

Experimental Section

Instrumentation. Electronic spectra were recorded on a Perkin-Elmer-Lambda 20 UV−vis spectrophotometer. IR spectra were obtained from a Perkin-Elmer 1320 infrared spectrophotometer. Proton NMR spectra were obtained on a 400 MHz JEOL spectrometer using $CDCl_3$ or CD_2Cl_2 as solvent. Chemical shifts are expressed in parts per million relative to residual $CHCl_3$ (7.258 ppm) or CH_2Cl_2 (5.3 ppm). FAB mass spectra were obtained on a JEOL SX-120/DA6000 spectrometer.

Materials. All NMR solvents were used as received. Dichloromethane was dried under calcium hydride and distilled under nitrogen before use. Silica gel (100−120 mesh) or neutral alumina or basic alumina (Merck, usually Brockmann grade III) was used for column chromatography. Di-*μ*-chloro-bis[dicarbonyl rhodium(I)] was purchased from Aldrich and was used as received. Various free base sapphyrins and rubyrins were synthesized and characterized as reported earlier from this laboratory.[5b]

X-ray Diffraction Analysis. ($C_{56}H_{32}N_4O_4Rh_2S_2$) 16. Small, golden-brown crystals were obtained by diffusion of methanol into a benzonitrile solution of **16**. The data crystal was a block with approximate dimensions of 0.20 × 0.18 × 0.06 mm^3. Crystal data and details of the data collection and structure refinement are listed in Table 2 and Supporting Information. The data were collected at 95(2) K on a Siemens SMART system, complete with a three-circle goniometer and CCD area detector.[20] The data collection nominally covered over a hemisphere of reciprocal space by a combination of three sets of

exposures; each set had a different ϕ angle for the crystal, and each exposure covered 0.3° in ω. The crystal to detector distance was 4.936 cm. Coverage of the unique set is over 97% complete to at least 26° in θ. Crystal decay was monitored by repeating the initial frames at the end of data collection and analyzing the duplicate reflections. No decay was observed. The data reduction was performed using SAINT, version 4, software.[21] The structure was solved by a combination of direct methods and refined on F^2 by full-matrix least-squares methods with anisotropic thermal parameters for the non-H atoms.[22] Hydrogen atoms were placed geometrically and refined with a riding model (including free rotation about C···C bonds for methyl groups) and with U(iso) constrained to be 1.2 times U(eq) of the carrier atom. The conventional $R(F)$ for 5494 reflections with $I > 2\sigma(I)$ was equal to 0.0384.

General Procedure for Syntheses of Rhodium Complexes. 1. (5,10,15,20-Tetraphenyl-26,28-dithiasapphyrinato)-25,29-dicarbonylrhodium(I) (7). Sapphyrin **4** (0.035 g, 0.049 mmol) was dissolved in alcohol-free dichloromethane (50 mL). Anhydrous sodium acetate (0.032 g, 0.49 mmol) was added to the solution followed by di-μ-chloro-bis[dicarbonylrhodium(I)] (0.019 g, 049 mmol), and the mixture was stirred for 20 min. The solvent was evaporated in vacuo, and the residue was chromatographed on a basic alumina column. The brown-red fraction eluted with petroleum ether/dichloromethane (3:1) gave a green solid identified as **7** (0.035 g, 82%), which decomposes above 250 °C. ^{1}H NMR (400 MHz, $CDCl_3$, 25 °C): δ 7.79(m, 4H), 7.92(m, 8H), 8.34-(m, 4H), 8.58(s, 2H), 8.62(m, 4H), 8.86(d, J = 4.4 Hz, 2H), 9.02(d, J = 4.4 Hz, 2H), 9.73(d, J = 5.2 Hz, 2H), 9.95(d, J = 5.2 Hz, 2H). UV−vis (CH_2Cl_2) λ_{max} (nm) ($\epsilon \times 10^{-4}$): 513 (11.23), 623 (1.29), 684 (0.28), 774 (0.15), 864 (1.33). IR (KBr) ν(CO): 1994, 2063 cm^{-1}. FAB-MS: m/z 872(30%) [M$^+$].

2. (5,10,15,20-Tetraphenyl-26,28-diselenasapphyrinato)-25,29-dicarbonylrhodium(I) (8). The above procedure was followed using **5** (0.030 g, 0.037 mmol), sodium acetate (0.030 g, 0.372 mmol), and di-μ-chloro-bis[dicarbonylrhodium(I)] (0.022 g, 0.056 mmol). The rhodium complex **8** was obtained in 62% (0.018 g) yield and decomposes above 250 °C. ^{1}H NMR (400 MHz, $CDCl_3$, 25 °C): δ 7.89(m, 8H), 7.94(m, 4H), 8.41(m, 4H), 8.53(m, 4H), 8.85(s, 2H), 8.99-(d, J = 4.4 Hz, 2H), 9.16(d, J = 4.4 Hz, 2H), 10.17(d, J = 5.2 Hz, 2H), 10.38(d, J = 5.2 Hz, 2H). UV−vis (CH_2Cl_2) λ_{max} (nm) ($\epsilon \times 10^{-4}$): 514 (5.56), 627 (0.84), 672 (0.39), 767 (0.15), 856 (0.82). IR (KBr) ν(CO): 2000, 2065 cm^{-1}. FAB-MS: m/z 968(20%) [(M + 2)$^+$].

3. (5,10,15,20-Tetramesityl-26,28-diselenasapphyrinato)-25,29-dicarbonylrhodium(I) (9). The above procedure was followed using the sapphyrin **6** (0.030 g, 0.031 mmol), sodium acetate (0.025 g, 0.310 mmol), and di-μ-chloro-bis[dicarbonyl rhodium(I)] (0.012 g, 0.031 mmol). The rhodium complex **9** was obtained in 57% (0.020 g) yield and decomposes above 260 °C. ^{1}H NMR (400 MHz, $CDCl_3$, 25 °C): δ 1.53(s, 6H), 1.65(s, 6H), 2.25(s, 6H), 2.34(s, 6H), 2.69(s, 6H), 2.73-(s, 6H), 7.30(s, 2H), 7.43(s, 2H), 7.45(s, 2H), 7.46(s, 2H), 8.80(s, 2H), 8.98(d, J = 4.8 Hz, 2H), 9.25(d, J = 4.0 Hz, 2H), 10.15(d, J = 5.6 Hz, 2H), 10.22(d, J = 4.4 Hz, 2H). UV−vis (CH_2Cl_2) λ_{max} (nm) ($\epsilon \times 10^{-4}$): 511(14.62), 623(2.41), 669(1.23), 763(0.53), 852(2.19). IR (KBr) ν(CO): 2002, 2068. FAB-MS: m/z 1136(35%) [(M + 2)$^+$].

4. (5,10,19,24-Tetramesityl-30,33-dioxarubyrinato)-31,34-*cis*-tetracarbonyldichlorodirhodium(I) (11) and (5,10,19,24-Tetramesityl-30,33-dioxarubyrinato)-31,34-*trans*-tetracarbonyldichlorodirhodium-(I) (12). These complexes were prepared by the reaction of **10** (0.044 g, 0.048 mmol) with sodium acetate (0.039 g, 0.480 mmol) and di-μ-chloro-bis[dicarbonylrhodium(I)] (0.047 g, 0.120 mmol) by a similar procedure described above. The crude product upon chromatographic separation on silica gel with dichloromethane gave the inseparable mixture of **11** and **12** as a green solid. Yield 0.03 g, 48%; decomposes above 280 °C. ^{1}H NMR (400 MHz, $CDCl_3$, 25 °C): δ −3.52(s, 2H), −2.36(d, J = 4.4 Hz, 2H), −2.15(d, J = 4.4 Hz, 2H), 1.70(s, 6H), 1.86(s, 6H), 2.21(s, 6H), 2.75(s, 12H), 2.74(s, 6H), 7.37(s, 2H), 7.42-(s, 4H), 7.67(s, 2H), 8.97(dd, J = 4.4 Hz, ^3J = 2 Hz, 2H), 9.20(d, J = 4.4 Hz, 2H), 9.28(d, J = 4.4 Hz, 2H), 10.90(dd, J = 4.4 Hz, ^3J = 2 Hz, 2H) for cis isomer. ^{1}H NMR (400 MHz, $CDCl_3$, 25 °C): δ −3.71-(s, 2H), −2.53(d, J = 4.4 Hz, 2H), −2.46(d, J = 4.4 Hz, 2H), 2.01(s, 6H), 2.03(s, 6H), 2.17(s, 6H), 2.69(s, 6H), 2.68(s, 12H), 7.38(s, 4H), 7.52(s, 2H), 7.59(s, 2H), 9.01(dd, J = 4.4 Hz, ^3J = 2 Hz, 2H), 9.26(d, J = 4.4 Hz, 2H), 9.37(d, J = 4.4 Hz, 2H), 11.29(dd, J = 4.4 Hz, ^3J = 2 Hz, 2H) for trans isomer. UV−vis (CH_2Cl_2) λ_{max} (nm) ($\epsilon \times 10^{-4}$): 527(9.16), 569(5.24)(sh), 702(0.71), 772(0.71), 860(0.31), 979(2.83). IR (KBr) ν(CO): 1993, 2068 cm^{-1}. FAB-MS: 1302(18%), [(M − 2)$^+$].

5. (5,10,19,24-Tetraphenyl-30,33-dithiarubyrinato)-29,34,31,32-tetracarbonyl-*cis*-dirhodium(I) (16), (5,10,19,24-Tetraphenyl-30,-33-dithiarubyrinato)-29,34,31,32-tetracarbonyl-*trans*-dirhodium-(I) (19), and (5,10,19,24-Tetraphenyl-30,33-dithiarubyrinato)-29,34-dicarbonylrhodium(I) (22). The above procedure was followed using rubyrin **13** (0.1 g, 0.129 mmol) with sodium acetate (0.105 g, 1.29 mmol) and di-μ-chloro-bis[dicarbonyl rhodium(I)] (0.1 g, 0.258 mmol). The solvent was evaporated, and the residue was chromatographed in the neutral alumina column. The first blue band that eluted with a petroleum ether and dichloromethane mixture (4:1) gave a golden-brown solid identified as **16** (yield, 0.005 g, 3.5%), which decomposes above 280 °C. ^{1}H NMR (400 MHz, $CDCl_3$, 25 °C): δ 7.87(m, 4H), 7.98(m, 8H), 8.02(d, J = 4.4 Hz, 4H), 8.12(d, J = 4.4 Hz, 4H), 8.66(m, 8H), 8.93(s, 4H). UV−vis (CH_2Cl_2) λ_{max} (nm) ($\epsilon \times 10^{-4}$): 579(8.54), 736-(0.66), 825(0.76), 1060(1.89). IR (KBr) ν(CO): 2003, 2069 cm^{-1}. FAB-MS: 1094(18%), [M$^+$]. The second violet band that eluted with a petroleum ether and dichloromethane mixture (2:1) gave a golden-brown solid in very low yield (<1%) and is identified as **19**. The last pink band that eluted with dichloromethane/ethyl acetate (9:1) gave a magenta solution. Upon evaporation a green solid was formed and was identified as **22** (yield, 0.02 g, 16.5%), which decomposes above 280 °C. ^{1}H NMR (400 MHz, $CDCl_3$, 25 °C): δ −5.88(brs, 1H), −2.81(brs, 2H), −2.48(brs, 2H), 7.80(m, 4H), 7.92(m, 8H), 8.05(m, 4H), 8.49-(brs, 2H), 8.54(m, 4H), 8.65(brs, 2H), 8.71(brs, 2H), 9.14(brs, 2H). UV−vis (CH_2Cl_2) λ_{max} (nm) ($\epsilon \times 10^{-4}$): 563(8.64), 704(0.89), 771-(0.58), 901(0.41), 1039(2.00). IR (KBr) ν(CO): 2008, 2069 cm^{-1}. FAB-MS: 937(31%), [M$^+$].

6. (5,10,19,24-Tetraphenyl-30,33-diselenarubyrinato)-29,34,31,-32-tetracarbonyl-*cis*-dirhodium(I) (17), (5,10,19,24-Tetraphenyl-30,-33-diselenarubyrinato)-29,34,31,32-tetracarbonyl-*trans*-dirhodium-(I) (20), and (5,10,19,24-Tetraphenyl-30,33-diselenarubyrinato)-29,34-dicarbonylrhodium(I) (23). These compounds were prepared similarly as above from **14** (0.1 g, 0.115 mmol), sodium acetate (0.095 g, 1.15 mmol), and di-μ-chloro-bis[dicarbonylrhodium(I)] (0.04 g, 0.23 mmol). In the chromatographic separation on neutral alumina, the first blue band that eluted with petroleum ether and dichloromethane (3:2) gave **17** as a golden-brown solid (yield 0.006 g, 5%), which decomposes above 290 °C. ^{1}H NMR (400 MHz, $CDCl_3$, 25 °C): δ 7.91(m, 4H), 8.02(m, 8H), 8.30(d, J = 4.4 Hz, 4H), 8.37(d, J = 4.4 Hz, 4H), 8.70-(m, 8H), 9.39(s, 4H). UV−vis (CH_2Cl_2) λ_{max} (nm) ($\epsilon \times 10^{-4}$): 595-(9.61), 695(0.55), 745(0.74), 835(1.29), 1076(2.47). IR (KBr) ν(CO): 2003, 2069 cm^{-1}. FAB-MS: 1188(32%), [M$^+$]. The second violet band that eluted with petroleum ether/dichloromethane (1:1) gave a brown solid that was identified as **20** (yield 0.004 g, 3%), which decomposes above 280 °C. ^{1}H NMR (400 MHz, $CDCl_3$, 25 °C): δ 3.42(d, J = 5.8 Hz, 1H), 3.44(d, J = 4.4 Hz, 1H), 3.72(d, J = 5.8 Hz, 1H), 3.78(d, J = 4.4 Hz, 1H), 7.50(m, 8H), 7.72(m, 4H), 7.79(m, 10H), 7.85(d, J = 4.8 Hz, 1H), 7.88(d, J = 4.8 Hz, 1H), 7.91(d, J = 4.8 Hz, 1H), 7.95(d, J = 4.4 Hz, 1H), 8.08(d, J = 4.4 Hz, 1H), 8.19(d, J = 4.4 Hz, 1H). UV−vis (CH_2Cl_2) λ_{max} (nm) ($\epsilon \times 10^{-4}$): 606(6.06), 757(0.74), 929-(0.97). IR (KBr) ν(CO): 2014, 2073 cm^{-1}. FAB-MS: 1188(10%) [M$^+$]. The fourth magenta band that eluted with 2% ethyl acetate in dichloromethane mixture gave **23** as a green solid (yield 0.04 g, 33%), which decomposes above 270 °C. ^{1}H NMR (400 MHz, $CDCl_3$, 25 °C): δ −2.81(brs, 2H), −2.76(brs, 2H), 7.81(m, 4H), 7.89(m, 8H), 8.00(m, 4H), 8.47(d, J = 6.0 Hz, 2H), 8.53(m, 4H), 8.58(d, J = 6.0 Hz, 2H), 8.63(brs, 2H), 8.95(brs, 2H). UV−vis (CH_2Cl_2) λ_{max} (nm) ($\epsilon \times 10^{-4}$): 564(13.3), 708(1.06), 775(0.96), 906(0.57), 1045(3.09); IR (KBr) ν(CO): 2003, 2069 cm^{-1}. FAB-MS: 1032(10%) [(M + 1)$^+$].

7. (5,10,19,24-Tetramesityl-30,33-diselenarubyrinato)-29,34,31,-32-tetracarbonyl-*cis*-dirhodium(I) (18), (5,10,19,24-Tetramesityl-30,-

(20) *SMART Software Reference Manual*; Siemens Analytical X-ray Instruments: WI, 1994.
(21) *SAINT, Software Reference Manual*, version 4; Siemens Analytical X-ray Instruments: WI, 1995.
(22) Sheldrick, G. M. *SHELXTL, Reference Manual*, version 5; Siemens Analytical X-ray Instruments: WI, 1994.

33-diselenarubyrinato)-29,34,31,32-tetracarbonyl-*trans*-dirhodium-(I) (21), and (5,10,19,24-Tetramesityl-30,33-diselenarubyrinato)-29,34-dicarbonylrhodium(I) (24). These compounds were prepared similarly as above from **15** (0.1 g, 0.097 mmol), sodium acetate (0.08 g, 0.97 mmol), and di-μ-chloro-bis[dicarbonyl rhodium(I)] (0.075 g, 0.194 mmol). The residue obtained from the reaction mixture was chromatographed on the silica gel column. The first blue band that eluted with a petroleum ether and dichloromethane mixture (4:1) gave **18** as a golden-brown solid (yield 0.004 g, 3%), which decomposes above 290 °C. ^{1}H NMR (400 MHz, $CDCl_3$, 25 °C): δ 2.09(s, 6H), 2.17(s, 6H), 2.39(s, 12H), 2.75(s, 12H), 7.40(s, 4H), 7.59(s, 4H), 8.61-(d, J = 4.4 Hz, 4H), 8.63(d, J = 4.4 Hz, 4H), 9.46(s, 4H). UV−vis (CH_2Cl_2) λ_{max} (nm) ($\epsilon \times 10^{-4}$): 592(7.31), 740(0.68), 819(1.06), 919-(0.25), 1052(2.06). IR (KBr) ν(CO): 2012, 2071 cm^{-1}. FAB-MS: 1358-(60%) [(M + 1)$^+$]. The second violet band that eluted with a petroleum ether and dichloromethane mixture (2:1) gave the **21** in <1% yield. The last pink band that eluted with dichloromethane gave **24** in 42% yield (0.055 g), which decomposes above 260 °C. ^{1}H NMR (400 MHz, $CDCl_3$, 25 °C): δ −1.82(d, J = 5.6 Hz, 2H), −1.49(d, J = 5.2 Hz, 2H), 1.31(s, 6H), 1.71(s, 6H), 2.63(s, 6H), 2.65(s, 6H), 2.70(s, 6H), 2.85(s, 6H), 7.15(s, 2H), 7.23(s, 2H), 7.46(s, 2H), 7.49(s, 2H), 8.62(d, J = 4.4 Hz, 2H), 8.68(d, J = 4.4 Hz, 2H), 9.13(d, J = 4.4 Hz, 2H), 9.38(d, J = 4.4 Hz, 2H). ^{1}H NMR (400 MHz, $CDCl_3$, −50 °C): δ −2.12(d, J = 4.8 Hz, 2H), −1.78(d, J = 4.8 Hz, 2H), −0.65(brs, 1H), 1.30(s, 6H), 1.68(s, 6H), 2.66(s, 6H), 2.67(s, 6H), 2.74(s, 6H), 2.89(s, 6H), 7.19(s, 2H), 7.28(s, 2H), 7.52(s, 2H), 7.54(s, 2H), 8.72(d, J = 4.0 Hz, 2H), 8.79(d, J = 4.0 Hz, 2H), 9.24(d, J = 4.4 Hz, 2H), 9.51(d, J = 4.0 Hz, 2H). UV−vis (CH_2Cl_2) λ_{max} (nm) ($\epsilon \times 10^{-4}$): 555(27.29), 698(2.61), 767(3.57), 890(1.68), 1028(6.68); IR (KBr) ν(CO): 1997, 2064 cm^{-1}. FAB-MS: 1201(25%) [(M + 2)$^+$].

Acknowledgment. This work was supported by grants from the Department of Science and Technology (DST) and the Council of Scientific and Industrial Research (CSIR), Government of India, New Delhi, to T.K.C. and a grant from the National Science Foundation to K.R.S. (Grant CHE-9702246). Purchase of the X-ray diffractometer equipment was made possible with grants from NSF (Grant CHE-95-27898), the W.M.Keck Foundation, and Syracuse University. T.K.C. is also grateful to the Alexander von Humboldt foundation for an equipment grant.

Supporting Information Available: Tables of crystal data, structure solution and refinement, atomic coordinates, bond lengths and angles, and anisotropic thermal parameters for compound **16**, FAB mass spectra for **7**, **11**, **12**, **17**, and **22**, IR spectra for **9**, **11**, **12**, **20**, and **22**, ^{1}H NMR ($CDCl_3$, −50 °C) spectra for **24**, and 2D ^{1}H−^{1}H COSY results for **7**, **17**, and **20**. This material is available free of charge via the Internet at http://pubs.acs.org.

IC000703H